Multiphonon hole trapping from first principles

F. Schanovsky,[a] W. Gös, and T. Grasser
Christian Doppler Laboratory for TCAD, Institute for Microelectronics, TU Wien, 1040 Wien, Austria

(Received 10 August 2010; accepted 6 December 2010; published 6 January 2011)

Nonradiative multiphonon capture of carriers into the gate dielectrics of metal-oxide-semiconductor systems and its involvement with the negative bias temperature instability is discussed. A simple method for the extraction of the line-shape function from an atomistic bulk defect model is suggested and applied to defect models in alpha quartz. Electronic structures are described using density functional theory. © *2011 American Vacuum Society.* [DOI: 10.1116/1.3533269]

I. INTRODUCTION

One of the most critical degradation effects observed in *p*-channel metal-oxide-semiconductor field-effect transistors (*p*-MOSFETs) is the negative bias temperature instability (NBTI).[1–3] It is encountered when a large negative bias is applied to the gate contact with all other terminals grounded. The amount of degradation strongly depends on the applied voltage and the device temperature.

We have recently suggested a new model for NBTI.[4] This model fits even experimental NBTI stress and relaxation data of increased complexity with very high accuracy and explains the behavior of small-scale MOSFETs under NBTI stress, observed by the time-dependent defect spectroscopy.[5] Our model explains the microscopic origin of the degradation as the capture of holes into oxide defects which causes a reorganization of the defect's atomic structure. This microscopic interpretation is different from the popular reaction-diffusion model for NBTI, which assumes the observed phenomena to be governed by the diffusion of some hydrogenic species.[1]

The temperature activated exchange of electrons and holes between the defect and the channel is described within the framework of nonradiative multiphonon theory (NMP).[6,7] The central actor within our model is an oxide defect—usually illustrated as an oxygen vacancy—which undergoes several well defined transitions in the course of degradation and recovery. These transitions require for a special configuration of the local minima and barriers of the defect's adiabatic potential energy surfaces in the different charge states. So far, these potentials have been empirically adjusted to fit the experimental data.

This work is a first step toward the analysis of the atomistic roots of our model. We focus on the examination of the hole-capture process by evaluating atomistic models of defect structures for their multiphonon properties using first-principles density functional theory (DFT) calculations. The defects selected for inspection are the oxygen vacancy and the hydrogen bridge. Both defects have been investigated before and show two stable configurations, as required by our model.[8–10] The oxygen vacancy has been previously suggested as the defect causing NBTI and other reliability issues such as radiation damage[10] or $1/f$ noise.[11] The hydrogen bridge has been proposed as the defect causing stress-induced leakage current.[9,12]

[a]Author to whom correspondence should be addressed; electronic mail: schanovsky@iue.tuwien.ac.at

II. MULTIPHONON TRANSITION THEORY

In semiconductor modeling, trapping of carriers is usually treated via the Shockley-Read-Hall model. This model characterizes a trap site using a (constant) capture cross section σ and a trap level E_T. For the transition process involved in NBTI it has been repeatedly demonstrated that this model provides an inappropriate description of the underlying physics.[13–15]

The description of electronic transition processes involving multiple ionic excitations of defects in semiconductors has been studied in detail by several authors.[6,7,16,17] The theory is based on a quantum-mechanical formulation, derived from perturbation theory and using the Franck-Condon principle. The nonradiative capture cross section from a free initial state i to a final localized state f is expressed as

$$\sigma_{if} = A_{if} f, \tag{1}$$

where A_{if} depends only on the electronic degrees of freedom and f—the so-called line-shape function (LSF)—describes the vibrational influence.

A_{if} is only briefly discussed here. It involves the crystal volume Ω, the electron thermal velocity $\langle v \rangle$, and the electronic matrix element

$$A_{if} = \frac{2\pi\Omega}{\hbar\langle v\rangle}\langle \phi_f | V' | \phi_i \rangle. \tag{2}$$

A_{if} cannot be obtained from an atomistic bulk defect calculation as the electronic matrix element requires the overlap of the electronic wave function of the initial and final states, which also includes the states in the silicon substrate. Usually, this quantity is estimated during a device simulation using a simple tunneling description such as the Wentzel-Kramers-Brillouin approximation[4,7] or overlaps of approximate electronic wave functions.[13]

The line-shape function f is used to explain the broadening of the optical absorption peaks of bulk defects[17] and reads

$$f = \operatorname{avg}_{\eta_i} \sum_{\eta_f} |\langle \eta_f | \eta_i \rangle|^2 \delta(E_{\eta_f} - E_{\eta_i}). \tag{3}$$

It comprises of a series of the Dirac peaks, weighted by the vibrational overlap $|\langle \eta_f | \eta_i \rangle|^2$. The thermal average extends over all vibrational states η_i associated with the initial electronic configuration ϕ_i, while the sum runs over all vibrational states η_f belonging to ϕ_f. E_{η_f} and E_{η_i} denote the total vibronic energy of the system associated with states η_f and η_i, respectively. In the following it is assumed that the energies used in Eq. (3) can be separated into a defect component $E^{\mathrm{d}}_{\eta_x}$ and a component E_{res} representing the reservoir, i.e., the spectrum of electronic states in the gate or the substrate sharing the same electronic matrix element,

$$E_{\eta_x} = E^{\mathrm{d}}_{\eta_x} + E_{\mathrm{res}}, \quad E_{\mathrm{res}} = \sum_i n_i E_i, \tag{4}$$

where i runs over all reservoir states. n_i and E_i denote the occupancy and the energy level of reservoir state i. For a hole-capture transition in which an electron from the defect is moved to the nth reservoir state, the occupation in the reservoir state E_n is raised by one, so the energy difference in Eq. (3) becomes

$$E_{\eta_f} - E_{\eta_i} = E^{\mathrm{d}}_{\eta_f} - E^{\mathrm{d}}_{\eta_i} + E_n. \tag{5}$$

The consequence of Eq. (5) is that now the line-shape function becomes dependent on the energy E_n of the hole that is trapped by the defect. Thus, we can rewrite Eq. (3) to obtain

$$f(E) = \operatorname{avg}_{\eta_i} \sum_{\eta_f} |\langle \eta_f | \eta_i \rangle|^2 \delta(E^{\mathrm{d}}_{\eta_f} - E^{\mathrm{d}}_{\eta_i} + E). \tag{6}$$

The effect of gate bias on the capture can be estimated by a simple model[18] in the limit of a nearly uncharged oxide. When the defect is approximated as an object of zero spatial extension and the hole state to be filled is approximated as localized at the oxide/semiconductor or oxide/metal interface, an electric field F in the oxide shifts the relative positions of the defect energies $E^{\mathrm{d}}_{\eta_x}$ and the reservoir states E_i by $e_0 x F$, where e_0 is the elementary charge and x is the effective distance between the defect and the insulator/semiconductor or insulator/metal interface. Consequently, if an electric field is applied, the shifted line-shape function $f(E+e_0 x F)$ has to be used.

III. CALCULATION OF THE LINE-SHAPE FUNCTION

The determining elements of the line-shape function are the overlaps of the vibrational wave functions and their corresponding defect energies. This, in turn, requires the calculation of the potential energy surfaces. In the present work we apply a series of approximations to devise a simple method for the extraction of the line-shape function from density functional bulk defect calculations.

In atomistic calculations, the system can be described by a single configuration vector $\vec{x}$ that holds all $3N$ coordinates of the N atoms under consideration. By setting the charge state of the system and applying a suitable optimization algorithm, one can obtain the optimum structure for the neutral ($\vec{x}_0$) and the charged ($\vec{x}_+$) defects along with the respective energies. The energies obtained from DFT will be denoted $E_0^{\mathrm{DFT}}(\vec{x})$ and $E_+^{\mathrm{DFT}}(\vec{x})$ for the neutral and the charged calculations, respectively.

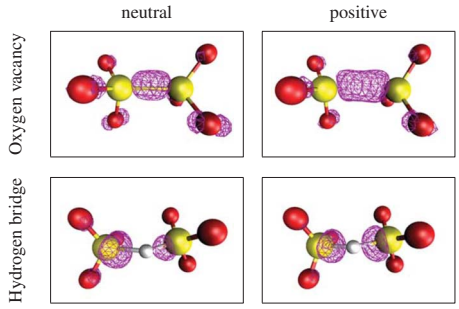

FIG. 1. (Color online) Optimized defect structures for both defects in the neutral as well as the positive state. The electron density of the localized Kohn-Sham eigenstate is shown as purple wireframe. The structural parameters were compared with those previously determined by Blöchl (Ref. 9) and showed excellent agreement.

The first simplification is the assumption of single mode coupling. It is assumed that only one vibrational mode contributes to the electronic transition, which is considered a first-order approximation.[7,17,19,20] The modal vector, the direction vector of the modal movement in the $3N$-dimensional space, is given as the direction from the initial (neutral) configuration to the final (charged) one,

$$\vec{m} = \vec{e}_{\vec{x}_+ - \vec{x}_0} = \sum_i c_i \vec{e}_i, \tag{7}$$

where the coefficients c_i are the components of the modal vector in the Cartesian base of the system. The associated modal mass is then given by

$$M = \sum_i c_i^2 M_i. \tag{8}$$

To further simplify the calculation, we assume parabolic energy surfaces for the neutral and charged states of the defect. The energy expressions of the neutral and positive states then become

$$E_0^{\mathrm{d}}(q) = \frac{M\omega_0^2}{2} q^2,$$

$$E_+^{\mathrm{d}}(q) = \frac{M\omega_+^2}{2}(q - q_{\mathrm{s}})^2 + E_{\mathrm{s}},$$

$$q_{\mathrm{s}} = |\vec{x}_0 - \vec{x}_+|, \quad E_{\mathrm{s}} = E_+^{\mathrm{DFT}}(\vec{x}_+) - E_0^{\mathrm{DFT}}(\vec{x}_0). \tag{9}$$

The parameters ω_0 and ω_+ are chosen such that

$$E_0^{\mathrm{d}}(q_{\mathrm{s}}) = E_0^{\mathrm{DFT}}(\vec{x}_+) \quad \text{and} \quad E_+^{\mathrm{d}}(0) = E_+^{\mathrm{DFT}}(\vec{x}_0) \tag{10}$$

in order to properly describe the relaxation energies in the approximate treatment. Consequently, the overlap integral becomes

TABLE I. Parameters of the defect potential energy surfaces [Eqs. (9)] extracted from DFT. The modal mass M and the modal frequency ω determine the curvature of the potential energy surface. E_s and q_s are the energetic and spatial shifts of the minima.

	M (amu)	ω_0 (rad s^{-1})	ω_+ (rad s^{-1})	E_s (eV)	q_s (Å)
Oxygen vacancy	24.66	7.02×10^{13}	4.48×10^{13}	2.68	0.56
Hydrogen bridge	16.33	3.88×10^{13}	4.04×10^{13}	−0.73	0.92

$$\langle \eta_f | \eta_i \rangle = \langle \omega_+, m | \omega_0, n \rangle, \tag{11}$$

where $|\omega, i\rangle$ is the ith eigenvector of the harmonic oscillator of frequency ω. Several analytic solutions for this integral can be found in the literature;[21–23] especially, simple expressions are available for the special case $\omega_0 = \omega_+$.[6,17,24] In the present work, we use the expression of Zapol,[21] which works for all cases.

IV. *AB INITIO* CALCULATIONS

The electronic structure is described with DFT using the gradient-corrected functional by Perdew, Burke, and Ernzerhof (PBE) functional. The calculations were performed using the Vienna *ab initio* simulation program (VASP).[25,26] The host lattice is an orthorhombic alpha-quartz supercell structure[9,27] containing 72 atoms. Alpha quartz was chosen because it is a well studied reference system for amorphous silica.[8,9,28] An oxygen vacancy is created by removing one oxygen atom from the system, the hydrogen bridge, by replacing an oxygen atom by a hydrogen atom. The wave functions are expanded in a plane-wave basis set up to 800 eV; the k space is sampled at the Γ point. The core electrons are represented using the projector augmented wave (PAW) method as parametrized in the VASP PAW database. The determination of the electron energies relative to the silicon bands follows the method described by Blöchl.[9]

V. RESULTS

Figure 1 shows the optimized defect structures in their neutral and positive states. The structural parameters were compared with Ref. 9 and showed excellent agreement. The parameters for Eqs. (9) as extracted for the two investigated defects from DFT are given in Table I.

The potential energy surfaces as calculated from Eqs. (9) using the parameters of Table I are shown in Fig. 2. One can estimate the activation barrier for the hole capture in the classical limit from the intersection of the two parabolas. It can be seen that the oxygen vacancy has to overcome a large (thermal) activation barrier of ≈2.7 eV in the transition from the neutral to the positive state. The hydrogen bridge in contrast shows a very small transition barrier and will be more stable in the positive state when the electron Fermi level is at silicon midgap.

The line-shape functions for both defects are shown in Fig. 3. The plain solution of Eq. (3) is a series of the weighted Dirac impulses as indicated in Fig. 3. Lifetime broadening[6] has been introduced in an empirical manner by the convolution of these impulses with a normal distribution of standard deviation k_BT. The hydrogen bridge is predicted to have its highest capture cross section near the silicon valence level, while the oxygen vacancy has its maximum capture weight approximately 0.9 eV above the SiO_2 valence level. At room temperature, a nonradiative transition of a

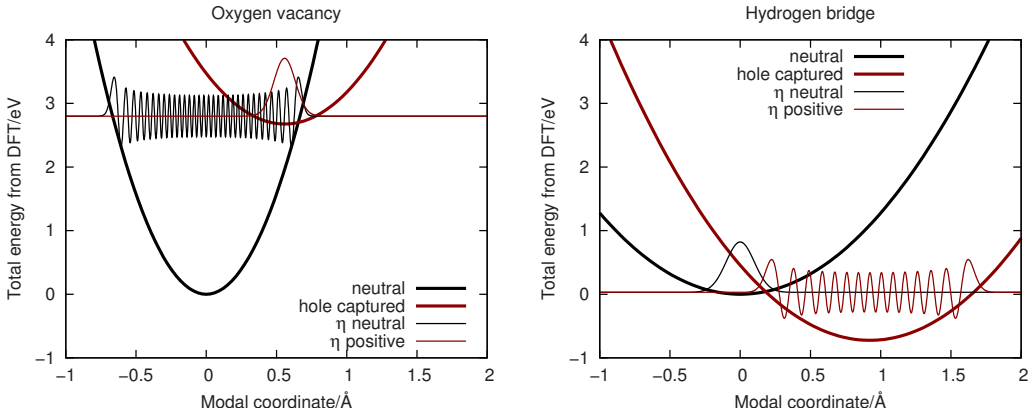

FIG. 2. (Color online) Potentials and selected vibrational wave functions for the oxygen vacancy and the hydrogen bridge for hole capture from the silicon valence level. The definition of the modal coordinate q is given in Eqs. (9). The activation energy in the classical limit can be estimated from the intersection of the neutral and positive potential energy surfaces.

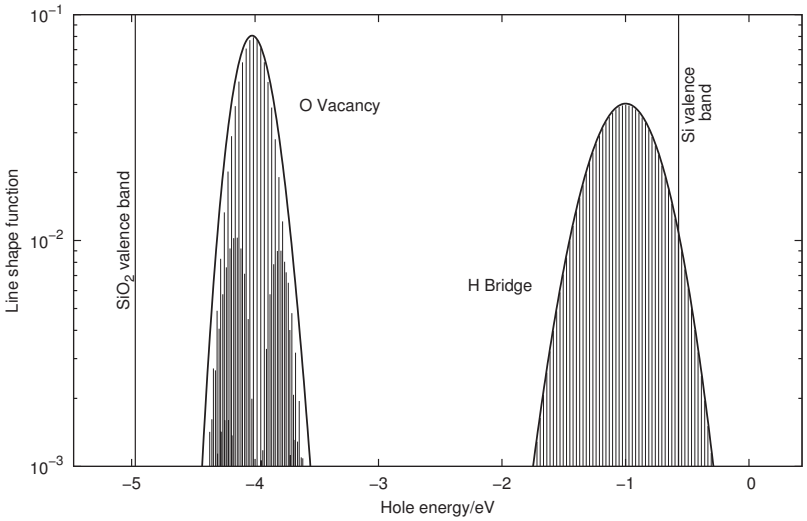

FIG. 3. Line-shape function at 300 K. Life-time broadening is simulated by smearing the Dirac peaks of Eq. (3) with a normal distribution of standard deviation k_BT.

hole residing near the Si valence band into this defect requires a deep position within the oxide and a high field to create significant overlap. For example, if the defect is 1 nm from the oxide, shifting the LSF by 1 eV would require a field of 10 MV/cm.

When considering NBTI, neither of the two investigated models appears to be in accord with experimental data. The thermodynamic transition level (see E_s in Table I) of the hydrogen bridge lies 0.73 eV above the silicon valence band. In a *p*-MOS transistor, the hydrogen bridge will thus favor the positive state for all bias conditions except accumulation. In NBTI experiments it will not show any degradation or recovery behavior whatsoever.

The oxygen vacancy, on the other hand, requires fields in the regime of 20 MV/cm to change the charge state of defects in a distance of 1 nm from the interface with an activation energy in the observed range of 0.5–1.0 eV.[5] For oxygen vacancies closer to the interface even higher fields are required. In thin oxides this would lead to vanishing NBTI, quite contrary to experimental evidence.

A thorough investigation is required to shed light on the dependence of the results on the employed methods, i.e., the DFT functional, the defect level alignment method, etc. Furthermore, the amorphous nature of the gate oxide, as well as the structural influence of the silicon substrate, has to be considered.

VI. CONCLUSIONS

The exchange of charge between oxide defects and the silicon substrate or the gate is heavily influenced by the vibrations of the defect structure. In the case of hole capture during NBT stress, this process is described by nonradiative multiphonon transition theory, which leads to a capture cross section dependent on temperature as well as on the energy of the hole to be trapped. Within the framework of the NMP theory, the influence of the vibrational degrees of freedom on the electronic transition is described by the line-shape function.

We have suggested a simple method to extract the LSF from density functional theory based atomistic defect models and have applied this method to the oxygen vacancy and the hydrogen bridge in crystalline SiO_2. This method is not limited to a specific material or electronic structure theory. Thus, it is also well suited for the investigation of defects in novel materials such as high-*k* dielectrics.

Both defect models do not fulfill the requirements of our NBTI model even if the usual error of ± 0.5 eV for the energies obtained from DFT calculations is considered. This may be due to the employed crystalline host structure model not capturing enough properties of the real oxide in MOS transistors or due to the method for alignment of the defect energies with the silicon valence level being inappropriate. Further investigations are required considering improved DFT functionals, as well as improved structural models of the MOS oxide.

ACKNOWLEDGMENTS

The authors thank A. Shluger, K. McKenna, G. Kresse, and P. E. Blöchl for valuable discussions. This work has received funding from the EC's FP7 grant Agreement No. 216436 (ATHENIS) and from the ENIAC MODERN Project No. 820379.

[1]K. O. Jeppson and C. M. Svensson, J. Appl. Phys. **48**, 2004 (1977).
[2]D. K. Schroder, Microelectron. Reliab. **47**, 841 (2007).
[3]T. Grasser, W. Goes, and B. Kaczer, *Defects in Microelectronic Materials and Devices* (Taylor & Francis, London/CRC, Cleveland, 2008), pp. 399–436.
[4]T. Grasser, B. Kaczer, W. Goes, T. Aichinger, P. Hehenberger, and M. Nelhiebel, Proceedings of the International Reliability Physics Symposium, 2009, pp. 33–44.
[5]T. Grasser, H. Reisinger, P.-J. Wagner, and B. Kaczer, Proceedings of the International Reliability Physics Symposium, 2010, pp. 16–25.
[6]C. H. Henry and D. V. Lang, Phys. Rev. B **15**, 989 (1977).
[7]S. Makram-Ebeid and M. Lannoo, Phys. Rev. B **25**, 6406 (1982).
[8]J. K. Rudra and W. B. Fowler, Phys. Rev. B **35**, 8223 (1987).
[9]P. E. Blöchl, Phys. Rev. B **62**, 6158 (2000).
[10]C. J. Nicklaw, Z.-Y. Lu, D. Fleetwood, R. Schrimpf, and S. Pantelides, IEEE Trans. Nucl. Sci. **49**, 2667 (2002).
[11]D. Fleetwood, H. Xiong, Z.-Y. Lu, C. Nicklaw, J. Felix, R. Schrimpf, and

S. Pantelides, IEEE Trans. Nucl. Sci. **49**, 2674 (2002).
[12]P. E. Blöchl and J. H. Stathis, Phys. Rev. Lett. **83**, 372 (1999).
[13]A. Palma, A. Godoy, J. A. Jemènez-Tejada, J. E. Carceller, and J. A. Lòpez-Villanueva, Phys. Rev. B **56**, 9565 (1997).
[14]N. Zanolla, D. Siprak, P. Baumgartner, E. Sangiorgi, and C. Fiegna, Proceedings of the Workshop on Ultimate Integration of Silicon, Udine, Italy, March 2008, pp. 137–140.
[15]M. Schulz, J. Appl. Phys. **74**, 2649 (1993).
[16]A. Schenk, J. Appl. Phys. **71**, 3339 (1992).
[17]K. Huang and A. Rhys, Proc. R. Soc. London, Ser. A **204**, 406 (1950).
[18]W. B. Fowler, J. K. Rudra, M. E. Zvanut, and F. J. Feigl, Phys. Rev. B **41**, 8313 (1990).
[19]A. Schenk, Acta Phys. Pol. A **69**, 813 (1986).
[20]A. M. Stoneham, Rep. Prog. Phys. **44**, 1251 (1981).
[21]B. Zapol, Chem. Phys. Lett. **93**, 549 (1982).
[22]F. Iachello and M. Ibrahim, J. Phys. Chem. A **102**, 9427 (1998).
[23]F. Ansbacher, Z. Naturforsch. A **14A**, 889 (1959).
[24]T. Markvart, J. Phys. C **14**, L895 (1981).
[25]G. Kresse and J. Furthmüller, Phys. Rev. B **54**, 11169 (1996).
[26]G. Kresse and D. Joubert, Phys. Rev. B **59**, 1758 (1999).
[27]E. Calabrese and W. Fowler, Phys. Rev. B **18**, 2888 (1978).
[28]A. S. Mysovsky, P. V. Sushko, S. Mukhopadhyay, A. H. Edwards, and A. L. Shluger, Phys. Rev. B **69**, 085202 (2004).